XBP1-mediated activation of the STING signaling pathway in macrophages contributes to liver fibrosis progression

Qi Wang, Qingfa Bu, Mu Liu, Rui Zhang, Jian Gu, Lei Li, Jinren Zhou, Yuan Liang, Wantong Su, Zheng Liu, Mingming Wang, Zhexiong Lian, Ling Lu, Haoming Zhou

Table of contents

Supplementary materials and methods

Cell isolation, culture and treatment

Hepatocytes, NPCs and liver macrophages were isolated as our previously study described.[1] Briefly, livers were perfused in situ via the portal vein with calcium- and magnesium-free Hanks balanced salt solution (HBSS) supplemented with 2% heat-inactivated FBS, followed by 0.27% collagenase IV (Sigma-Aldrich, St Louis, MO, USA). Perfused livers were dissected, and teased through 70 μm nylon mesh cell strainers (BD Biosciences, San Diego, CA, USA). Liver cells were suspended in 20 mL DMEM with 10% FBS and divided into NPCs, including liver macrophages, and hepatocytes as follows. Liver cells were centrifuged at 50 g for 2 min, and the supernatant was collected. This step was repeated three times, and the NPCs in the supernatant were collected by centrifugation at 800 g for 5 min. NPCs were then suspended and allowed to attach to cell culture plates in DMEM with 10% FBS, 10 mM N-(2-hydroxyethyl)piperazine-N′-ethanesulfonic acid, 2 mM GlutaMax, penicillin (100 U/mL), and streptomycin (100 μg/mL) for 15 min at 37 ℃. Non-adherent cells were removed by replacement of the culture medium. The adherent cells were used for further ex vivo experiments. Liver macrophages were cultured in vitro for 6 h, and then cells or supernatants were collected for further analysis. The purity of liver macrophages was approximately 80%. Primary hepatocytes were pelleted after centrifugation at 50 g for 2 min. Cells were resuspended in 20 mL of 40% cold Percoll solution (P1644, Sigma) and centrifuged at 150 g for 7 min. The pelleted hepatocytes were washed once with DMEM plus 10% FBS, suspended in plating medium (Williams E medium with hepatocyte thawing and plating supplement pack), and plated in collagen type I-coated plates for 3 h. Maintenance medium (Williams E medium with hepatocyte maintenance supplement pack) was used for cultures overnight or longer.

Bone marrow cells were isolated from mouse femurs and tibias. Cells were cultured in DMEM supplemented with 10% FBS and 20% L929-conditioned medium for 7 days as previously described.[2,3] Bone marrow-derived macrophages (BMDMs) were then replated and cultured overnight in new culture dishes for further experiments. The negative control and specific *Bnip3* siRNAs were purchased (RiboBio, Guangzhou, China). The sequences of small interfering RNA (siRNA) were as follows: *Bnip3*-siRNA 5'-CAGCCUCCGUCUCUAUUUATTT-3'. BMDM transfection was conducted with Lipofectamine 3000 (Invitrogen, Carlsbad, CA, USA) according

to the manufacturer's specifications. Lentiviral plasmids (GenePharma, Shanghai, China) expressing *Nlrp3* and *Tmem173*, short hairpin RNAs (shRNAs) against *Irf3* (5'-CCGGCCAATGTGAACAACTTCCTAACTCGAGTTAGGAAGTTGTTCACATTGGTTTTTG-3'), and vectors (designated LV-*Nlrp3*, LV-*Tmem173*, Sh-*Irf3* and vector) were used to transfect BMDMs. After 48 h, the cells were treated with 100 ng/ml LPS (Sigma, St. Louis, MO, USA), which is a major component of the outer membrane of gram-negative bacteria and a potent activator of macrophages, and incubated for an additional 6 h with or without ATP (4 mM, 1 h) treatment in vitro to simulate in vivo injury and inflammation. BMDMs isolated from $Xbp1^{M\text{-}KO}$ mice were treated with 5,6-dimethylxanthenone-4-acetic acid (DMXAA; a STING activator; 75 μg/mL) and subjected to collection of conditioned media (CM). BMDMs isolated from $Xbp1^{FL/FL}$ mice were stimulated with LPS with or without toyocamycin (1 μM) or tunicamycin (2 μg/ml) for 6 h. BMDMs isolated from $Xbp1^{FL/FL}$ mice were treated with KIN1148 (10 μM) with or without LPS stimulation for 6 h.

HSCs were isolated according to the previously published method.[4] Briefly, primary hepatic stellate cells (HSCs) were isolated from the liver of mice. After intubation in the portal vein, the livers were perfused *in situ* with Ca^{2+}-free Hank's balanced saline solution (HBSS) at 37°C for 15 min and then perfused with the solution containing 0.05% collagenase and Ca^{2+} for 15 min at a flow rate of 10 mL/min. Perfused livers were minced, filtered through 70 M cell strainer (BD Bioscience), and centrifuged at 50 g for 3 min. The supernatant was further centrifuged at 500 g for 10 min, resuspended in Ficoll plus Percoll (1:10, GE Healthcare), and centrifuged at 1400 g for 17 min. HSCs were collected from the interface. Then, primary mouse HSCs were incubated with BMDM-CM and assayed for HSC activation status in the absence or presence of transforming growth factor β1 (TGFβ1; 8 ng/mL for 24 hours).[2]

The mitochondria-specific antioxidant MitoTEMPO (MedChemExpress, New Jersey, USA) was purchased to treat cells. Cells were treated with MitoTEMPO (50 μM) prior to LPS administration. IRE1α inhibitor 4μ8C (MedChemExpress, New Jersey, USA) was purchased to treat cells. Cells were treated with 4μ8C (100 μM) prior to LPS administration. For mtDNA depletion assays, EtBr (MedChemExpress, New Jersey, USA) was purchased to treat cells. BMDMs (0.5×10^5 cells) were grown in a six-well plate and treated with 400 ng/ml EtBr, which was refreshed every 48 h in the medium. On day 6, BMDMs were collected and seeded for experiments.

RNA sequencing assay

BMDMs were isolated from *Xbp1*$^{FL/FL}$ and *Xbp1*$^{M\text{-}KO}$ mice and lysed in TRIzol reagent (Invitrogen, Carlsbad, CA) after LPS stimulation for 6 h. Total RNA was extracted from the cells by TRIzol reagent (Invitrogen). cDNA libraries were constructed for each pooled RNA sample using the NEBNext® Ultra™ Directional RNA Library Prep Kit from Illumina according to the manufacturer's instructions. The functions of the differentially expressed genes were analyzed by KEGG analysis. Raw data were deposited in the GEO database (GSE206693).

Chromatin immunoprecipitation (ChIP) assays

The ChIP analysis was carried out using ChIP Assay Kit (Abcam, MA). Briefly, BMDMs were treated with 1% formaldehyde for 10 min to crosslink proteins and chromatin. The reaction was stopped by adding 0.125M glycine for 5 min. Cells were washed with ice cold PBS and then resuspended with ChIP lysis buffer for 10 min. Cell lysates were centrifuged to pellet the nuclei. The cell nuclei were resuspended in nuclei lysis buffer and then subjected to sonication for 15 min. Purified chromatin was analysed on a 1.5 % agarose gel to analyze DNA fragment size. The sheared chromatin was immunoprecipitated with IRF3 (Cell Signaling Technology, MA, USA) or sXBP1 (Cell Signaling Technology, MA, USA) antibody overnight. As a control, the normal IgG was used as a replacement for IRF3 or sXBP1 antibody. The antibody/chromatin samples were mixed with protein A sepharose beads. Protein-DNA complexes were washed and eluted followed by a cross-link reversal step, and the resulting DNA was purified. DNA from each immunoprecipitation reaction was examined by PCR. The primer for the IRF3-responsive region of *Nlrp3* promoter: forward: 5'-ACGCTCTGTCTACAGCTTCTTG-3', reverse: 5'-GGAGGATGAGCAAACACCACTC-3'. The primer for the sXBP1-responsive region of *Bnip3* promoter: forward: 5'-CTCCGAGCACTGTAAGAAAGCA-3', reverse: 5'-TGAGCCATGTCACCAGACTGAA-3'.

Luciferase assays

The *Bnip3* promoter: luciferase reporter plasmid (*Bnip3* luciferase) was constructed in pGL3 luciferase vector (Promega, WI) according to the manufacturer's instructions. BMDMs were transfected with pGL3-*Bnip3*-luciferase vector. After transfection for 6h, the cells were washed and

transfected with Ad-*sXbp1* or Ad-CON.[5,6] 48h later, the cells were lysed with Passive Lysis Buffer, and the transcriptional activity was measured using a luciferase assay system according to the manufacturer's instructions (Promega).

Histological, immunohistochemical and immunofluorescence analysis

Liver specimens were fixed in 10% buffered formalin and embedded in paraffin. Sections of liver tissues (4 μm) were stained with H&E. Liver tissue sections (4 μm thickness) were stained with Sirius red to determine the degree of collagen deposition. For immunohistochemical staining, primary antibodies against α-SMA or Ly6G (Cell Signaling Technology, MA, USA) were added and incubated with liver tissue sections. Horseradish peroxidase (HRP)-conjugated secondary antibodies were used. Then, 3,3'-diaminobenzidine tetrachloride was used. The nuclei were counterstained with hematoxylin. The expression of XBP1s, STING, NLRP3 and CD68 in human liver tissues was determined by immunofluorescence staining with anti-rabbit XBP1s mAbs (Cell Signaling Technology, MA, USA), anti-rabbit STING mAbs (Abcam, Cambridge, UK), anti-rat NLRP3 mAbs (Invitrogen, Carlsbad, USA) and anti-mouse CD68 mAbs (Abcam, Cambridge, UK). The expression of CD11b in murine liver tissues was determined by immunofluorescence staining with anti-rabbit CD11b mAbs (Cell Signaling Technology, MA, USA). Then, liver tissues were incubated with goat anti-rabbit Texas Red-conjugated immunoglobulin G (IgG), goat anti-rabbit Texas Green-conjugated immunoglobulin G (IgG), goat anti-rat Texas Red-conjugated IgG or goat anti-mouse Texas Green-conjugated IgG (Sigma, St. Louis, MO, USA) secondary antibodies. The expression of STING and NLRP3 in BMDMs was determined by immunofluorescence staining with anti-rabbit STING pAbs (Invitrogen, Carlsbad, USA) and anti-rat NLRP3 mAbs (Invitrogen, Carlsbad, USA). Next, BMDMs were incubated with Anti-rabbit IgG (H+L), (Alexa Fluor® 488 Conjugate) or Anti-rat IgG (H+L), (Alexa Fluor® 647 Conjugate) (Cell Signaling Technology, MA, USA) secondary antibodies. DAPI was used to stain the nuclei. The slides were washed twice with phosphate-buffered saline (PBS) and observed with confocal microscopy (ZEISS, Oberkochen, Germany) in accordance with the manufacturer's instructions. Positive cells were counted blindly in 10 high-power fields (HPF)/section (×400).

Measurement of mitochondrial membrane potential and mtDNA release

Cells were stained with tetramethylrhodamine (TMRM) (Invitrogen, Carlsbad, USA) as described in the manufacturer's protocol. Cells were loaded with 200 nM TMRM for 30 min and then washed three times with PBS. TMRM fluorescence was measured by confocal microscopy (ZEISS, Oberkochen, Germany). Cells were stained with PicoGreen (Invitrogen, Carlsbad, USA) and MitoTracker (Invitrogen, Carlsbad, USA) according to the manufacturer's instructions. Laser power was kept as low as possible to avoid bleaching the signal.

Mitochondrial isolation and DNA extraction

Macrophage mitochondria were isolated using a mitochondria isolation kit (Thermo Scientific, MA, USA). mtDNA was purified using a QIAamp DNA mini kit (Qiagen, Dusseldorf, Germany) according to the manufacturer's instructions.

Detection of mtDNA in cytosolic extracts

Digitonin extracts from BMDMs were generated largely as previously described.[7,8] *Xbp1*$^{FL/FL}$ or *Xbp1*$^{M\text{-}KO}$ BMDMs (1×10^7 cells) were exposed to 4OHT for 72 h and divided into two equal aliquots; one aliquot was resuspended in 500 ml of 50 mM NaOH and boiled for 30 min to solubilize the DNA. Fifty milliliters of 1 M Tris-HCl pH 8 was added to neutralize the pH, and these extracts served as normalization controls for total mtDNA. The second aliquot was resuspended in approximately 500 ml of buffer containing 150 mM NaCl, 50 mM HEPES pH 7.4, and 15-25 mg/ml digitonin (Beyotime, Shanghai, China). The homogenates were incubated end-over-end for 10 min to allow selective plasma membrane permeabilization and then centrifuged at 980 g for 3 min 3 times to pellet intact cells. The cytosolic supernatants were transferred to fresh tubes and centrifuged at 17,000 g for 10 min to pellet any remaining cellular debris, yielding cytosolic preparations that were free of nuclear, mitochondrial and ER contamination. DNA was then isolated from these pure cytosolic fractions using QIAQuick Nucleotide Removal Columns (Qiagen, Dusseldorf, Germany). Quantitative PCR was performed on both whole-cell extracts and cytosolic fractions using nuclear DNA primers (*Tert*) and mtDNA primers (*Dloop*, *Cytb*, *Nd4*), and the CT values obtained for the mtDNA abundance in whole-cell extracts served as the normalization controls for the mtDNA values obtained from the cytosolic fractions. Using this digitonin method, no nuclear *Tert* DNA was detected in the cytosolic fractions, indicating that nuclear lysis did not occur. Nuclear DNA encoding

Tert was used for normalization.

Determination of oxidative stress

ROS production was determined by analyzing the fluorescence intensity of 2',7'-dichlorodihydrofluorescein diacetate (DCFH-DA) (Beyotime, Shanghai, China) and MitoSOX (Invitrogen, Carlsbad, USA) staining. In brief, BMDMs were incubated with DCFH-DA or MitoSOX at 37°C for 30 min and then analyzed by confocal microscopy (ZEISS, Oberkochen, Germany) according to the manufacturer's instructions.

Antioxidative enzyme activity

MnSOD activity assays were performed with a kit (BioVision, California, USA) according to the manufacturer's instructions. Before measuring the enzymatic activity of MnSOD, mitochondria were isolated from cells using a mitochondria isolation kit (Pierce, Illinois, USA) according to the manufacturer's instructions.

Transmission electron microscopy

Transmission electron microscopy was used to analyze BMDMs according to the manufacturer's instructions. In brief, cells were treated with 1% OsO4, dehydrated with ethanol, embedded in Epon and then fixed with 2.5% glutaraldehyde at 4°C overnight. The embedded cells were further stained with 0.3% lead citrate and imaged with an electron microscope (Hitachi, Tokyo, Japan; 5000× magnification).

Western blot analysis

Proteins were extracted from liver tissues and cells with ice-cold lysis buffer (50 mM Tris, 150 mM NaCl, 1% sodium deoxycholate, 0.1% sodium dodecyl sulfate, 1% Triton-100). The following primary antibodies were added and incubated with the membranes: XBP1 rabbit mAbs (Abcam, Cambridge, UK), α-SMA, Collagen I, TIMP1, NLRP3, cleaved caspase-1 (C-caspase-1), total caspase-1 (pro-caspase-1), cleaved IL-1β (IL-1β), cGAS, STING, p-TBK1, TBK1, p-IRF3, IRF3, LC3B, p62, β-actin rabbit mAbs, total IL-1β (pro-IL-1β), Parkin mouse mAbs (Cell Signaling Technology, MA, USA), TLR4 (Proteintech, Wuhan, China), p-IRE1α, PINK1 rabbit pAbs, and

BNIP3 rabbit mAbs (Abcam, Cambridge, UK). The reactions were detected with HRP-conjugated goat anti-rabbit IgG (Cell Signaling Technology, MA, USA) or goat anti-mouse IgG (Cell Signaling Technology, MA, USA) secondary antibodies.

Real-time qPCR

Total RNA was purified from liver tissues or BMDMs with TRIzol reagent (Invitrogen, Carlsbad, CA, USA), and a cDNA Synthesis Kit (Roche, Indianapolis, IN, USA) was used to perform reverse transcription. The target genes were amplified with a LightCycler 480 and SYBR Green 1 Master Mix (Roche, Indianapolis, IN, USA). Quantitative real-time PCR was repeated three times. The results were uniformly normalized to β-actin. The primers used in our study are presented in Table S6.

Enzyme-linked immunosorbent assay (ELISA)

The levels of TNF-α, IL-1β, and IL-10 (Abcam, Cambridge, UK) in serum or cell culture supernatants were quantified with ELISA kits according to the manufacturer's protocols.

Flow cytometry

PBMCs were isolated by gradient centrifugation using Ficoll-Paque Plus (GE Healthcare Life Science, Chicago, USA). The human-specific antibodies or isotype controls used for flow cytometry were as follows: STING (APC) (Novus, Colorado, USA), XBP1 (APC) (Novus, Colorado, USA), CD11b (PE) (Abcam, Cambridge, UK). The cells were examined on a FACS Canto flow cytometer and analyzed using FlowJo 10.0.7 software.

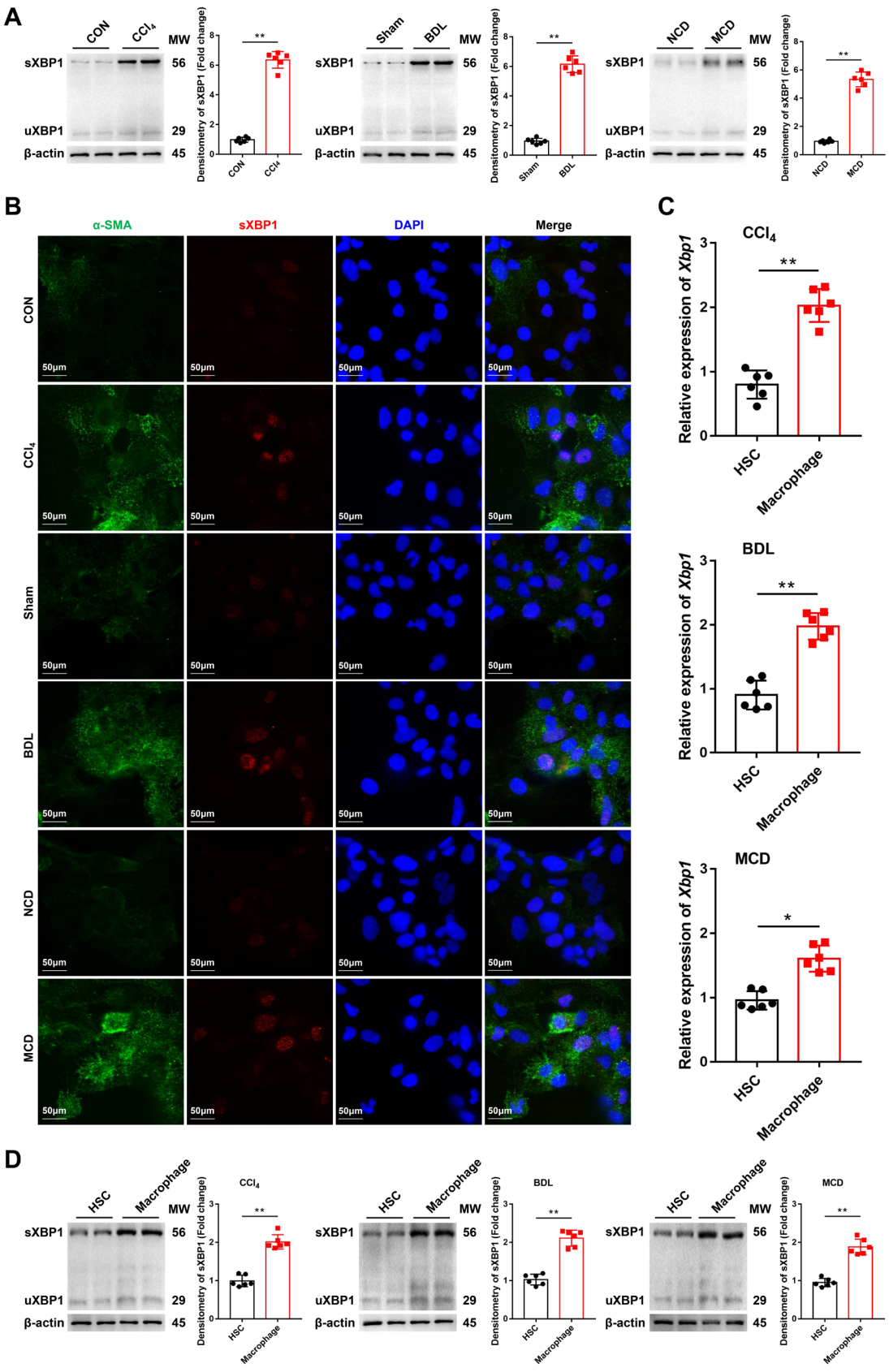

Fig. S1 XBP1 activation is primarily enhanced in macrophages than hepatic stellate cells in fibrotic liver tissues.

(A) The protein levels of XBP1 in macrophages isolated from mice with or without CCl_4-, BDL- and MCD-induced liver fibrosis. (B) Dual immunofluorescence staining of spliced XBP1 (red) and α-SMA (green) in primary stellate cells isolated from mice with CCl_4-, BDL- and MCD-induced liver fibrosis. (C) The gene expression levels of *Xbp1* in primary stellate cells and macrophages isolated from mice with CCl_4-, BDL- and MCD-induced liver fibrosis; n = 6 mice/group. (D) The protein levels of XBP1 in primary stellate cells and macrophages isolated from mice with CCl_4-, BDL- and MCD-induced liver fibrosis; n = 6 mice/group. Mean ± SD; Statistical significance was assessed by Student's t test; $^{**}P< 0.01$; $^{*}P< 0.05$.

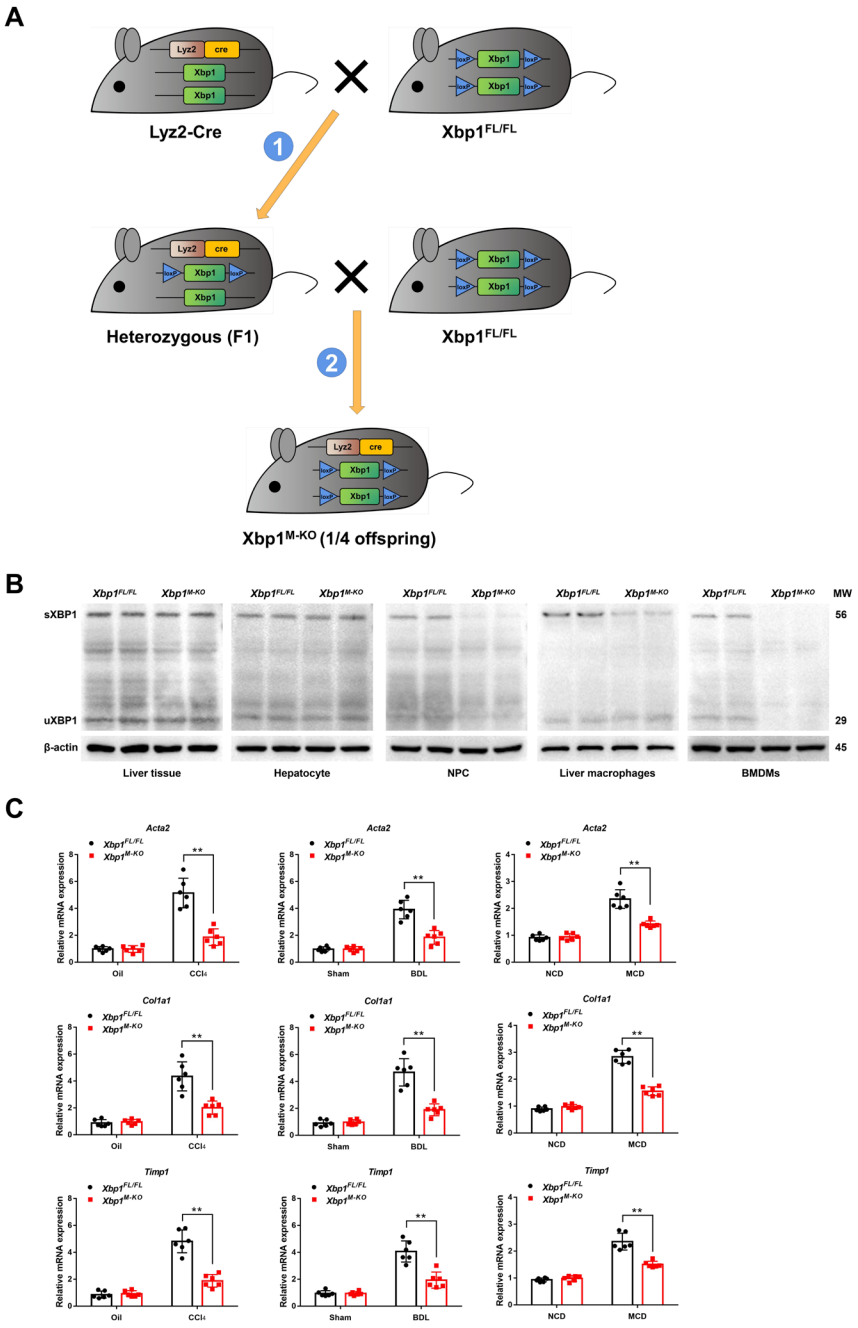

Fig. S2 Myeloid *Xbp1* deficiency ameliorates experimental liver fibrosis.

(A) Generation flow chart of myeloid-specific *Xbp1* deficient mice. (B) Western blot-assisted XBP1 expression profiles in liver tissues, hepatocytes, NPCs, liver macrophages and BMDMs from *XBP1*$^{FL/FL}$ and *XBP1*$^{M-KO}$ mice. (C) The gene expression levels of *Acta2*, *Col1a1* and *Timp1* in liver tissues from mice with CCl_4-, BDL- and MCD-induced liver fibrosis were examined by quantitative real-time PCR; n = 6 mice/group. Mean ± SD; Statistical significance was assessed by ANOVA; $^{**}P< 0.01$.

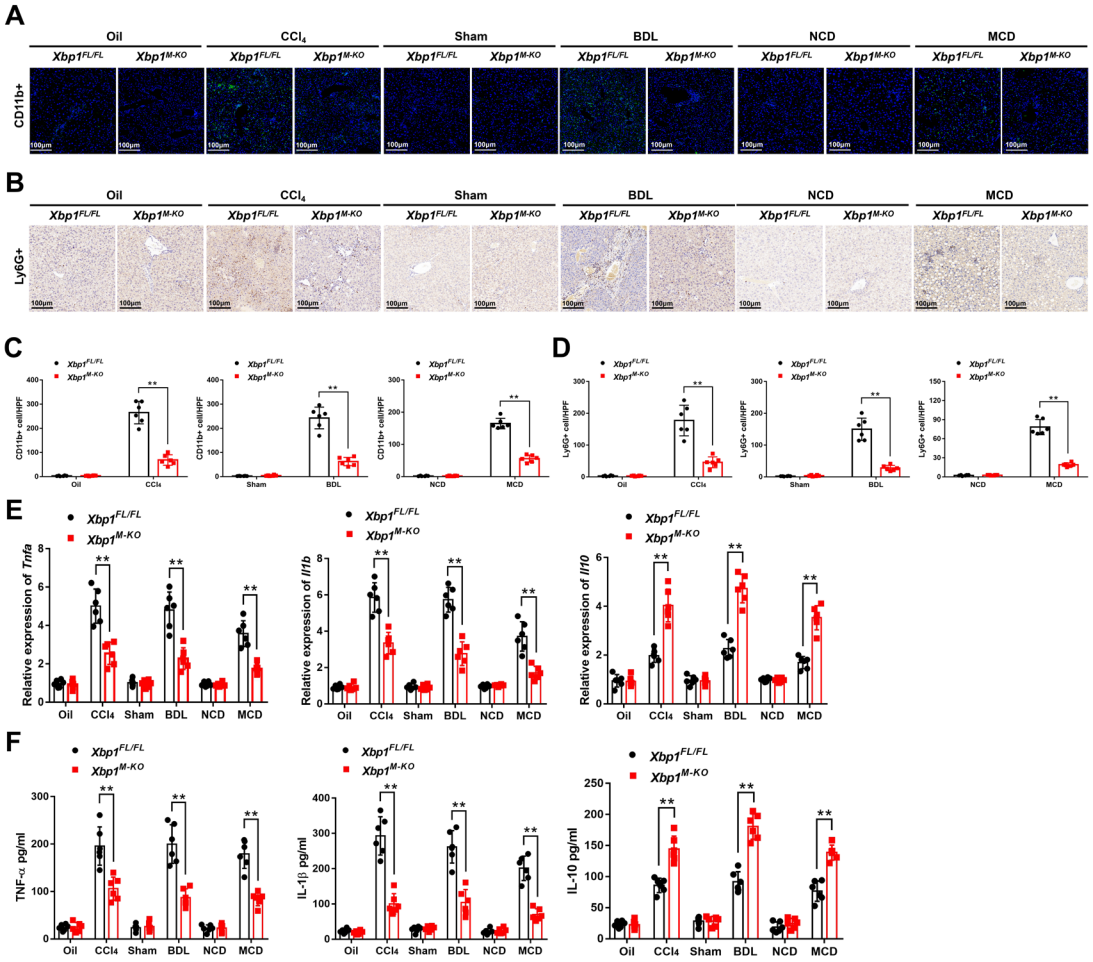

Fig. S3 Myeloid *Xbp1* deficiency attenuates inflammation in mice fibrotic livers.

(A) Immunofluorescence was performed to examine $CD11b^+$ macrophages in liver tissues from mice with CCl_4-, BDL- and MCD-induced liver fibrosis. Scale bar=100 μm. Representative of six mice/group. (B) Immunohistochemistry was performed to examine $Ly6G^+$ neutrophils in liver tissues from mice with CCl_4-, BDL- and MCD-induced liver fibrosis. Scale bar=100 μm. Representative of six mice/group. (C) $CD11b^+$ cells were quantified in the different groups (original magnification ×200); n = 6 mice/group. (D) $Ly6G^+$ cells were quantified in the different groups (original magnification ×200); n = 6 mice/group. (E) The gene expression levels of *Tnfa*, *Il1b*, and *Il10* in liver tissues from mice with CCl_4-, BDL- and MCD-induced liver fibrosis were examined by quantitative real-time PCR; n = 6 mice/group. (F) Serum levels of inflammatory cytokines, including TNF-α, IL-1β, and IL-10, were measured by ELISA; n = 6 mice/group. Mean ± SD; Statistical significance was assessed by ANOVA; $^{**}P< 0.01$; $^{*}P< 0.05$.

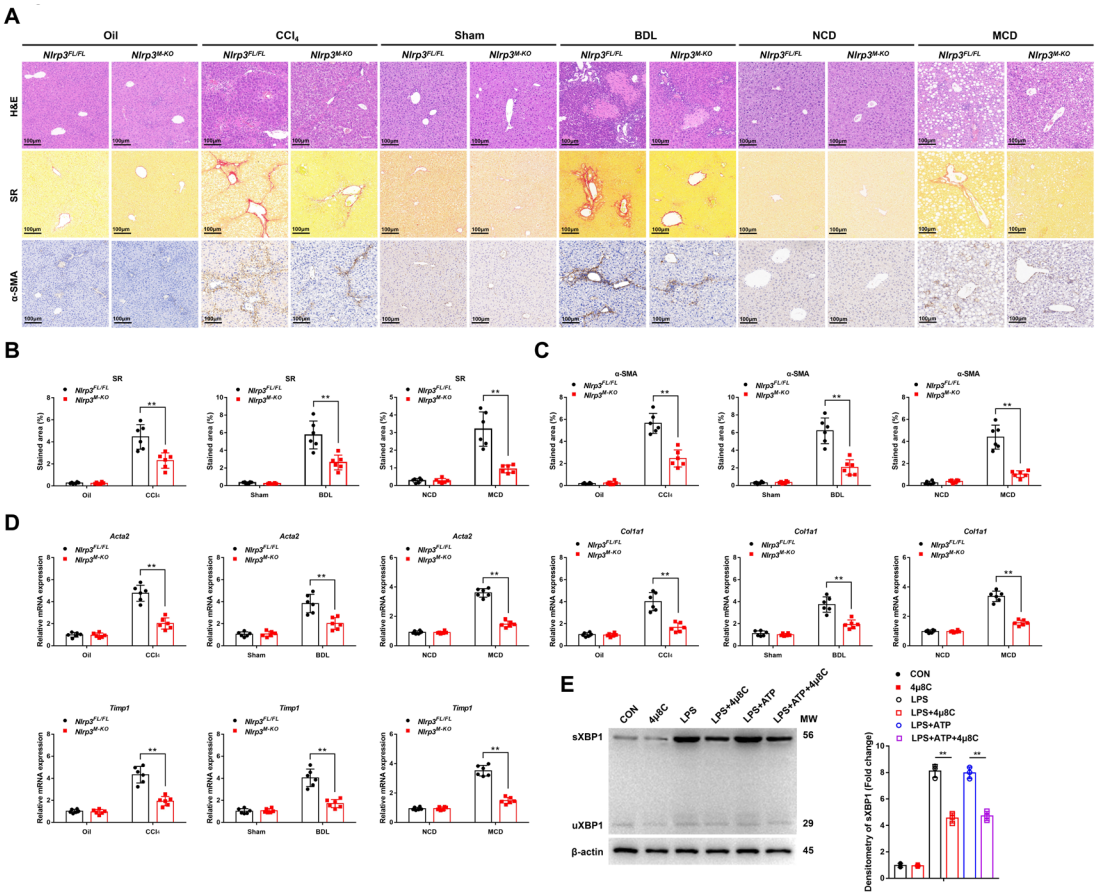

Fig. S4 Myeloid *Nlrp3* deficiency ameliorates experimental liver fibrosis.

(A) Male *Nlrp3*$^{FL/FL}$ and *Nlrp3*$^{M\text{-}KO}$ mice were subjected to CCl_4-, BDL- or MCD-induced experimental fibrosis, and the livers were collected and subjected to H&E staining, Sirius red staining, and α-SMA immunohistochemical analysis. Scale bar=100 μm. Representative of six mice/group. (B,C) The proportions of Sirius red-positive and α-SMA-positive areas were quantified; n=6 mice/group. (D) The gene expression levels of *Acta2*, *Col1a1*, and *Timp1* in liver tissues from *Nlrp3*$^{FL/FL}$ and *Nlrp3*$^{M\text{-}KO}$ mice with CCl_4-, BDL- and MCD-induced liver fibrosis were examined by quantitative real-time PCR; n = 6 mice/group. (E) The protein levels of XBP1 in *Xbp1*$^{FL/FL}$ BMDMs treated with LPS, LPS+4μ8C, LPS+ATP or LPS+ATP+4μ8C. Mean ± SD; Statistical significance was assessed by ANOVA; $^{**}P< 0.01$; $^{*}P< 0.05$.

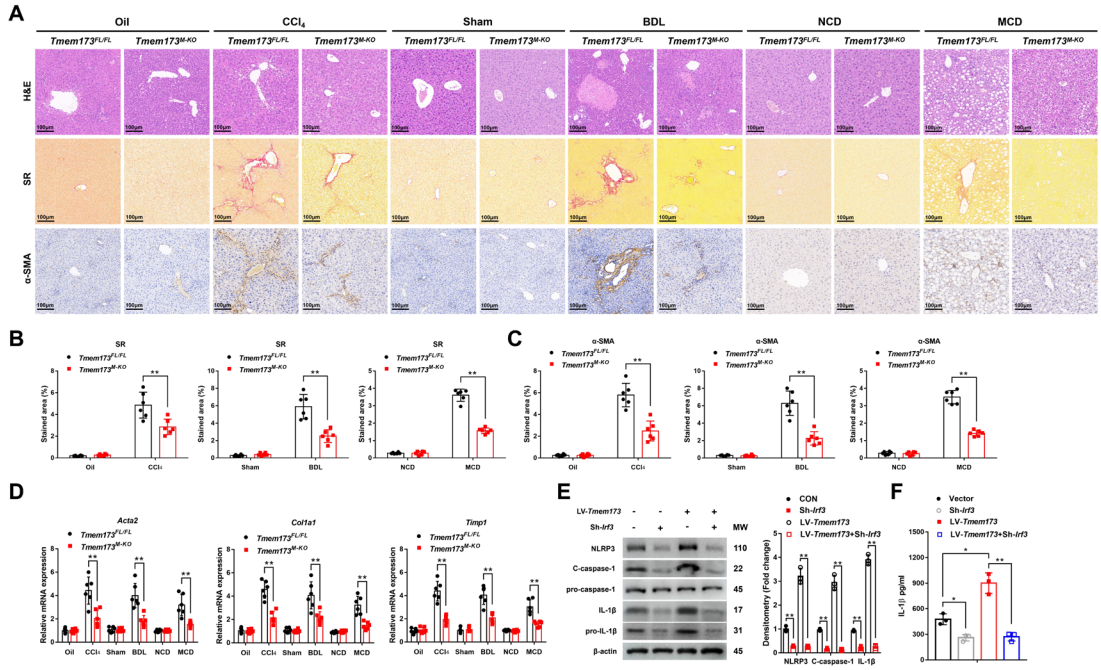

Fig. S5 Myeloid *Tmem173* deficiency ameliorates experimental liver fibrosis.

(A) Male *Tmem173*$^{FL/FL}$ and *Tmem173*$^{M\text{-}KO}$ mice were subjected to CCl_4-, BDL- or MCD-induced experimental fibrosis, and the livers were collected and subjected to H&E staining, Sirius red staining and α-SMA immunohistochemical analysis. Scale bar=100 μm. Representative of six mice/group. (B,C) The proportions of the Sirius red-positive and α-SMA-positive areas were quantified; n=6 mice/group. (D) The gene expression levels of *Acta2*, *Col1a1*, and *Timp1* in liver tissues from *Tmem173*$^{FL/FL}$ and *Tmem173*$^{M\text{-}KO}$ mice with CCl_4-, BDL- and MCD-induced liver fibrosis were examined by quantitative real-time PCR; n = 6 mice/group. (E) Western blot was performed to examine intracellular NLRP3, cleaved caspase-1, pro-caspase-1, cleaved IL-1β, and pro-IL-1β protein levels in LPS+ATP-stimulated *Xbp1*$^{M\text{-}KO}$ BMDMs transfected with LV-*Tmem173* or Sh-*Irf3*. (F) IL-1β expression in the supernatant of LPS+ATP-stimulated *Xbp1*$^{M\text{-}KO}$ BMDMs transfected with LV-*Tmem173* or Sh-*Irf3* was measured by ELISA; n = 3/group. Mean ± SD; Statistical significance was assessed by ANOVA; ***P*< 0.01; **P*< 0.05.

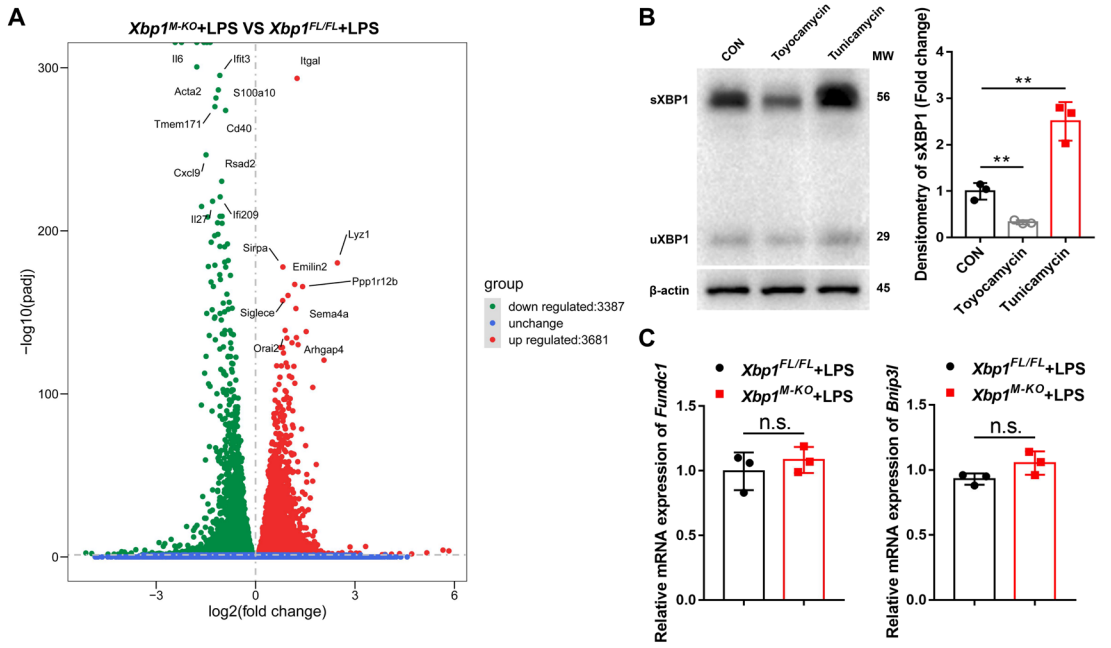

Fig. S6 Volcano plot of all differentially expressed genes, the protein levels of XBP1 in macrophages and the gene levels of *Fundc1* and *Bnip3l* in macrophages.

(A) Volcano plot of all differentially expressed genes in LPS-stimulated $Xbp1^{M\text{-}KO}$ VS $Xbp1^{FL/FL}$ BMDMs. (B) Western blot was performed to analyze the levels of sXBP1 in $Xbp1^{FL/FL}$ BMDMs treated with toyocamycin or tunicamycin. (C) The gene levels of *Fundc1* and *Bnip3l* in LPS-stimulated $Xbp1^{FL/FL}$ or $Xbp1^{M\text{-}KO}$ BMDMs; n = 3/group. Mean ± SD; Statistical significance was assessed by Student's t test or ANOVA; $^{**}P< 0.01$.

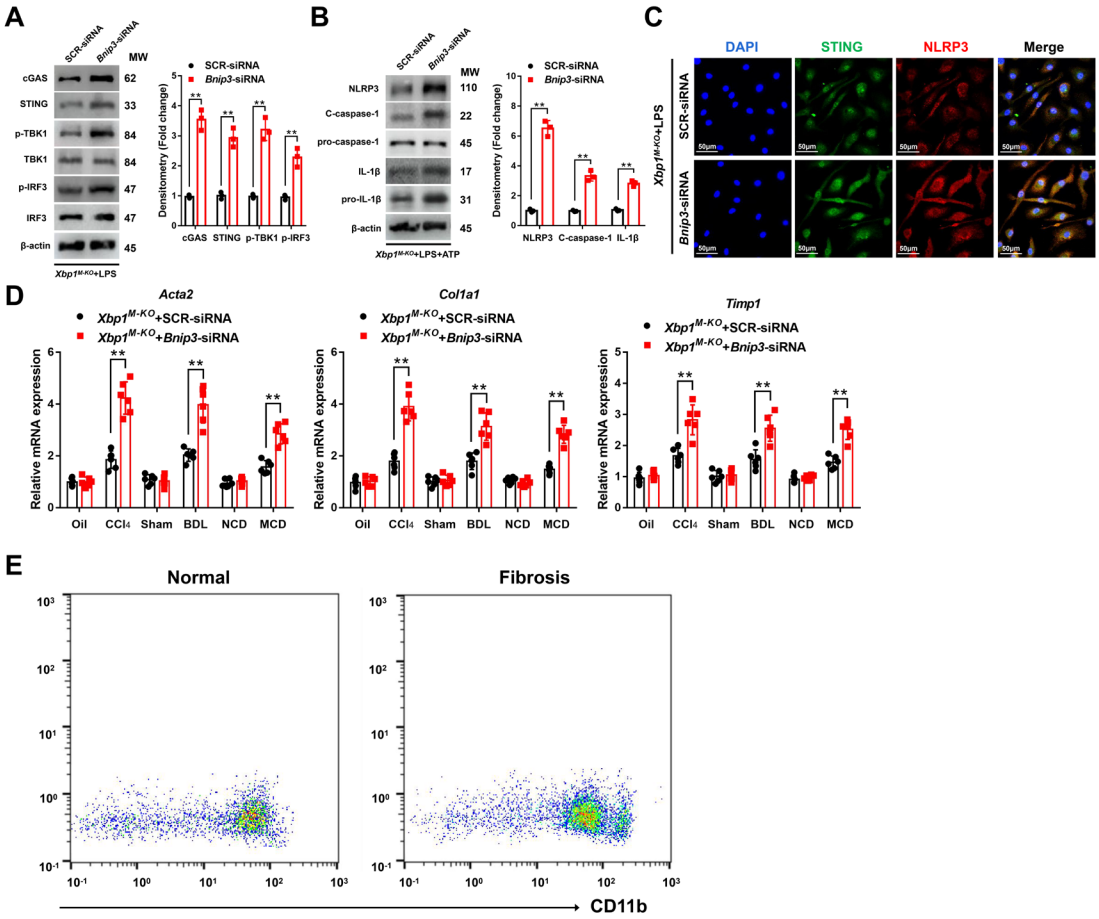

Fig. S7 BNIP3-mediated mitophagy activation is responsible for decreased mtDNA release and STING-NLRP3 activation in *Xbp1*-deficient macrophages.

(A) Western blot was performed to analyze the levels of cGAS, STING, p-TBK1, TBK1, p-IRF3 and IRF3 in *Xbp1*$^{M\text{-}KO}$ BMDMs transfected with SCR-siRNA or *Bnip3*-siRNA. Statistical analysis was carried out using Student's t test. (B) Western blot was performed to examine NLRP3, cleaved caspase-1, pro-caspase-1, cleaved IL-1β, and pro-IL-1β protein levels in LPS+ATP-stimulated *Xbp1*$^{M\text{-}KO}$ BMDMs transfected with SCR-siRNA or *Bnip3*-siRNA. Statistical analysis was carried out using Student's t test. (C) Immunofluorescence staining showing STING (green) and NLRP3 (red) colocalization in LPS-stimulated *Xbp1*$^{M\text{-}KO}$ BMDMs transfected with SCR-siRNA or *Bnip3*-siRNA. (D) The gene expression levels of *Acta2*, *Col1a1*, and *Timp1* in liver tissues from mice with liver fibrosis were examined by quantitative real-time PCR; n = 6 mice/group; one-way ANOVA. (E) The fluorescence minus one control (CD11b staining) for XBP1 staining of human PBMCs. Mean ± SD; Statistical significance was assessed by Student's t test or ANOVA; $^{**}P< 0.01$; $^{*}P< 0.05$.

Table S1: Demographic information of the study population.

Clinical manifestation	Patients with hepatic hemangioma	Patients with hepatic fibrosis					
Fibrosis stage	Normal	Mild fibrosis			Advanced fibrosis		
		HBV(1-4)	HCV(1-2)	NASH(1-2)	HBV(5-6)	HCV(3-4)	NASH(3-4)
Number	42	14	12	7	5	11	5
Age(years)	46.36±7.29	47.93±8.91	50.42±9.00	54.00±6.91	51.20±8.03	51.91±8.44	47.20±7.36
BMI(kg/m^2)	24.94±3.45	24.36±2.97	23.61±2.76	33.84±6.54	24.80±3.37	24.79±3.43	34.10±6.05
Sex(male/female)	14/28	8/6	7/5	5/2	3/2	7/4	4/1
Serum TB (umol/L)	8.66±3.04	21.02±5.13	19.41±5.90	18.09±4.49	23.99±6.71	22.79±5.85	22.18±3.61
Serum ALT (U/L)	20.06±7.41	64.06±15.31	69.67±15.75	62.46±14.44	86.01±16.00	79.98±16.29	68.16±14.32
Serum AST (U/L)	22.03±6.95	63.29±17.59	62.33±19.06	62.89±14.74	77.45±13.59	82.63±15.47	68.78±21.23
Serum ALB (g/L)	42.13±4.96	38.54±3.80	40.04±3.90	37.82±4.09	35.41±1.92	35.55±3.51	35.56±3.61

Hepatic fibrosis stage in patients with HBV infection was defined as Ishak fibrosis score, 1-4 for Mild fibrosis, 5-6 for Advanced fibrosis.[9-10] Hepatic fibrosis stage in patients with HCV infection was defined as Metavir score, 1-2 for Mild fibrosis, 3-4 for Advanced fibrosis.[11-13] Hepatic fibrosis stage in patients with NASH was defined as NAFLD activity score, 1-2 for Mild fibrosis, 3-4 for Advanced fibrosis.[14-16] Quantitative variables are in mean±SD. HBV, Hepatitis B virus; HCV, Hepatitis C virus; NASH, non-alcoholic steatohepatitis; BMI, Body mass index; ALB, albumin; ALT, alanine aminotransferase; AST, aspartate aminotransferase; TB, total bilirubin.

Table S2: Hepatic fibrosis stage in patients with HBV infection was defined as Ishak fibrosis score.

Fibrosis stage (Ishak)	1	2	3	4	5	6
Number	5	4	2	3	1	4
Age(years)	50.20±8.84	48.50±10.45	46.5±9.50	44.33±3.30	53	50.75±8.93
BMI(kg/m^2)	24.99±2.97	24.28±2.90	24.34±3.93	23.43±1.86	26.29	24.43±3.68
Sex(male/female)	3/2	2/2	1/1	1/2	1/0	3/1
Serum TB (umol/L)	18.16±4.09	20.13±3.80	24.28±2.80	24.80±5.88	22.57	24.34±7.46
Serum ALT (U/L)	54.75±9.91	68.96±12.72	68.23±8.50	70.28±20.96	90.68	84.84±17.70
Serum AST (U/L)	51.58±12.22	65.14±19.19	72.73±4.66	74.06±16.77	87.6	74.91±14.10
Serum ALB (g/L)	39.73±4.60	38.48±3.89	38.11±1.56	36.90±2.27	35.99	35.27±2.12

Table S3: Hepatic fibrosis stage in patients with HCV infection was defined as Metavir score.

Fibrosis stage (Metavir)	1	2	3	4
Number	9	3	5	6
Age(years)	51.22±8.52	48±9.93	50.40±7.17	53.17±9.17
BMI(kg/m^2)	23.41±3.08	24.20±1.23	24.36±3.50	25.16±3.32
Sex(male/female)	5/4	2/1	3/2	4/2
Serum TB (umol/L)	18.43±4.68	22.35±7.89	21.38±6.88	23.96±4.51
Serum ALT (U/L)	66.14±16.39	80.25±6.05	79.80±15.26	80.13±17.10
Serum AST (U/L)	56.55±17.15	79.69±13.02	84.23±4.78	81.30±20.39
Serum ALB (g/L)	40.21±4.44	39.51±1.17	36.07±4.54	35.12±2.23

Table S4: Hepatic fibrosis stage in patients with NASH was defined as NAFLD activity score.

Fibrosis stage (NAS)	1	2	3	4
Number	3	4	2	3
Age(years)	59.33±1.25	50±6.71	46±4	48±8.83
BMI(kg/m^2)	34.21±6.95	33.57±6.19	33.69±7.22	34.37±5.11
Sex(male/female)	1/2	3/1	2/0	3/0
Serum TB (umol/L)	16.82±2.37	19.04±5.38	22.78±0.82	21.78±4.56
Serum ALT (U/L)	58.84±7.45	65.18±17.49	68.37±3.50	68.02±18.26
Serum AST (U/L)	56.78±8.27	67.48±16.73	67.41±18.33	69.70±22.90
Serum ALB (g/L)	39.98±1.05	36.19±4.72	35.86±3.46	35.37±3.70

Table S5: Primer sequences for the amplification. (H, denotes human and M, denotes mice).

Gene	Forward Primer (5′ → 3′)	Reverse Primer (5′ → 3′)
H-XBP1	5’-CCCTCCAGAACATCTCCCCAT-3’	5’-ACATGACTGGGTCCAAGTTGT-3’
H-STING	5’-AGCATTACAACAACCTGCTACG-3’	5’-GTTGGGGTCAGCCATACTCAG-3’
H-NLRP3	5’-GATCTTCGCTGCGATCAACAG-3’	5’-CGTGCATTATCTGAACCCCAC-3’
H-β-ACTIN	5’-CATGTACGTTGCTATCCAGGC-3’	5’-CTCCTTAATGTCACGCACGAT-3’
M-Xbp1	5’-AGCAGCAAGTGGTGGATTTG-3’	5’-GAGTTTTCTCCCGTAAAAGCTGA-3’
M-Nlrp3	5’-ATTACCCGCCCGAGAAAGG-3’	5’-TCGCAGCAAAGATCCACACAG-3’
M-Bnip3	5’-TCCTGGGTAGAACTGCACTTC-3’	5’-GCTGGGCATCCAACAGTATTT-3’
M-Fundc1	5’-CCCCCTCCCCAAGACTATGAA-3’	5’-CCACCCATTACAATCTGAGTAGC-3’
M-Bnip3l	5’-ATGTCTCACTTAGTCGAGCCG-3’	5’-CTCATGCTGTGCATCCAGGA-3’
M-Acta2	5’-GTCCCAGACATCAGGGAGTAA-3’	5’-TCGGATACTTCAGCGTCAGGA-3’
M-Col1a1	5’-GCTCCTCTTAGGGGCCACT-3’	5’-CCACGTCTCACCATTGGGG-3’
M-Timp1	5’-CGAGACCACCTTATACCAGCG-3’	5’-ATGACTGGGGTGTAGGCGTA-3’
M-Tnfa	5’-CCCTCACACTCAGATCATCTTCT-3’	5’-GCTACGACGTGGGCTACAG-3’
M-Il1b	5’-GCAACTGTTCCTGAACTCAACT-3’	5’-ATCTTTTGGGGTCCGTCAACT-3’
M-Il6	5’-CTGCAAGAGACTTCCATCCAG-3’	5’-AGTGGTATAGACAGGTCTGTTGG-3’
M-Il10	5’-GCTCTTACTGACTGGCATGAG-3’	5’-CGCAGCTCTAGGAGCATGTG-3’
M-Cxcl10	5’-CCAAGTGCTGCCGTCATTTTC-3’	5’-GGCTCGCAGGGATGATTTCAA-3’
M-D-loop	5’-AATCTACCATCCTCCGTGAAACC-3’	5’-TCAGTTTAGCTACCCCCAAGTTTAA-3’
M-mt-Cytb	5’-AGTAGACAAAGCCACCTTGA-3’	5’-CCGCGATAATAAATGGTAAG-3’
M-mt-Nd4	5’-AACGGATCCACAGCCGTA-3’	5’-AGTCCTCGGGCCATGATT-3’

M-mt-Tert	5'-CTAGCTCATGTGTCAAGACCCTCTT-3'	5'-GCCAGCACGTTTCTCTCGTT-3'
M-β-Actin	5'-GGCTGTATTCCCCTCCATCG-3'	5'-CCAGTTGGTAACAATGCCATGT-3'

Supplementary references

Author names in bold designate shared co-first authorship.

[1] **Zhou H, Wang H,** Ni M, Yue S, Xia Y, Busuttil RW, et al. Glycogen synthase kinase 3β promotes liver innate immune activation by restraining AMP-activated protein kinase activation. J Hepatol 2018;69:99-109.

[2] **Luo X, Li H, Ma L,** Zhou J, Guo X, Woo SL, et al. Expression of STING Is Increased in Liver Tissues From Patients With NAFLD and Promotes Macrophage-Mediated Hepatic Inflammation and Fibrosis in Mice. Gastroenterology 2018;155:1971-1984.e1974.

[3] **Rao J, Cheng F, Zhou H,** Yang W, Qiu J, Yang C, et al. Nogo-B is a key mediator of hepatic ischemia and reperfusion injury. Redox Biol 2020;37:101745.

[4] Koo JH, Lee HJ, Kim W, Kim SG. Endoplasmic Reticulum Stress in Hepatic Stellate Cells Promotes Liver Fibrosis via PERK-Mediated Degradation of HNRNPA1 and Up-regulation of SMAD2. Gastroenterology 2016;150:181-193.e188.

[5] Wang ZV, Deng Y, Gao N, Pedrozo Z, Li DL, Morales CR, et al. Spliced X-box binding protein 1 couples the unfolded protein response to hexosamine biosynthetic pathway. Cell 2014;156:1179-1192.

[6] Schiattarella GG, Altamirano F, Kim SY, Tong D, Ferdous A, Piristine H, et al. Xbp1s-FoxO1 axis governs lipid accumulation and contractile performance in heart failure with preserved ejection fraction. Nat Commun 2021;12:1684.

[7] West AP, Khoury-Hanold W, Staron M, Tal MC, Pineda CM, Lang SM, et al. Mitochondrial DNA stress primes the antiviral innate immune response. Nature 2015;520:553-557.

[8] Holden P, Horton WA. Crude subcellular fractionation of cultured mammalian cell lines. BMC Res Notes 2009;2:243.

[9] Sun Y, Zhou J, Wang L, Wu X, Chen Y, Piao H, et al. New classification of liver biopsy assessment for fibrosis in chronic hepatitis B patients before and after treatment. Hepatology 2017;65:1438-

1450.

[10] Sun Y, Wu X, Zhou J, Meng T, Wang B, Chen S, et al. Persistent Low Level of Hepatitis B Virus Promotes Fibrosis Progression During Therapy. Clin Gastroenterol Hepatol 2020;18:2582-2591.e2586.

[11] **Patin E, Kutalik Z,** Guergnon J, Bibert S, Nalpas B, Jouanguy E, et al. Genome-wide association study identifies variants associated with progression of liver fibrosis from HCV infection. Gastroenterology 2012;143:1244-1252.e1212.

[12] Cacoub P, Carrat F, Bédossa P, Lambert J, Pénaranda G, Perronne C, et al. Comparison of non-invasive liver fibrosis biomarkers in HIV/HCV co-infected patients: the fibrovic study--ANRS HC02. J Hepatol 2008;48:765-773.

[13] Konerman MA, Mehta SH, Sutcliffe CG, Vu T, Higgins Y, Torbenson MS, et al. Fibrosis progression in human immunodeficiency virus/hepatitis C virus coinfected adults: prospective analysis of 435 liver biopsy pairs. Hepatology 2014;59:767-775.

[14] Jung J, Loomba RR, Imajo K, Madamba E, Gandhi S, Bettencourt R, et al. MRE combined with FIB-4 (MEFIB) index in detection of candidates for pharmacological treatment of NASH-related fibrosis. Gut 2021;70:1946-1953.

[15] Harrison SA, Rossi SJ, Paredes AH, Trotter JF, Bashir MR, Guy CD, et al. NGM282 Improves Liver Fibrosis and Histology in 12 Weeks in Patients With Nonalcoholic Steatohepatitis. Hepatology 2020;71:1198-1212.

[16] Siddiqui MS, Yamada G, Vuppalanchi R, Van Natta M, Loomba R, Guy C, et al. Diagnostic Accuracy of Noninvasive Fibrosis Models to Detect Change in Fibrosis Stage. Clin Gastroenterol Hepatol 2019;17:1877-1885.e1875.